Available online at www.sciencedirect.com

ScienceDirect

Journal of Nuclear Materials 373 (2008) 94–102

journal of nuclear materials

www.elsevier.com/locate/jnucmat

In situ observation of lithium hydride hydrolysis by DRIFT spectroscopy

Roy P. Awbery [a,*], Duncan A. Broughton [a], S.C. Tsang [b]

[a] *Chemical Technology Division, AWE plc, Reading, Berks RG7 4PR, UK*
[b] *School of Chemistry, Reading University, UK*

Received 6 February 2007; accepted 1 May 2007

Abstract

Polycrystalline LiH was studied *in situ* using diffuse reflectance infrared Fourier transform (DRIFT) spectroscopy to investigate the effect water vapour has on the rate of production of the corrosion products, particularly LiOH. The reaction rate of the formation of surface LiOH was monitored by measurement of the hydroxyl (OH) band at 3676 cm^{-1}. The initial hydrolysis rate of LiH exposed to water vapour at 50% relative humidity was found to be almost two times faster than LiH exposed to water vapour at 2% relative humidity. The hydrolysis rate was shown to be initially very rapid followed by a much slower, almost linear rate. The change in hydrolysis rate was attributed to the formation of a coherent layer of LiOH on the LiH surface. Exposure to lower levels of water vapour appeared to result in the formation of a more coherent corrosion product, resulting in effective passivation of the surface to further attack from water.

PACS: 82.65.+r; 33.20.Ea

1. Introduction

Lithium hydride (LiH) has a high affinity for water vapour, resulting in a surface layer of lithium hydroxide (LiOH) and/or lithium oxide (Li_2O) on exposure to trace quantities of moisture [1]. Consequently, even though this material is handled under dry atmosphere conditions (∼10 ppm H_2O), a surface layer of hydrolysis products can always be detected [2]. LiH is known to continually outgas hydrogen (H_2) due to a solid-state reaction between LiH and LiOH [3,4], but H_2 production is significantly increased during hydrolysis [5,6]. Hydrolysis of the bulk material results in significant swelling due to an increase in molar volume as the LiOH/Li_2O content increases [4,7]. The swelling and production of H_2 has serious implications for fuel storage cells and containment vessels. The swelling can lead to breach of containment and further exposure to moist air and H_2 can lead to hydriding corrosion in reactive metal components. It is therefore important to understand how LiH hydrolysis occurs to be able to predict the extent of hydrolysis under specific conditions of moisture exposure.

Many of the hydrolysis studies on LiH have been conducted under high vacuum conditions and at elevated temperatures. These conditions simplified the studies by removing the added complication of constant and rapid hydrolysis from external water sources. Controlled water vapour dosing was also employed where discreet quantities of water were introduced to the sample prior to monitoring the hydrolysis reactions. However, LiH hydrolysis under ambient conditions has been far less studied [2], and even less so for conditions that are more analogous to those employed for the storage and handling of LiH [8] where constant water vapour exposure can occur. The limited studies under ambient conditions has primarily been due to the difficulty of controlling the reaction environments and because the hydrolysis reactions tend to be very fast.

---

* Corresponding author. Tel.: +44 118 982 7020.
E-mail address: roy.p.awbery@awe.co.uk (R.P. Awbery).

0022-3115/$ - see front matter Crown Copyright © 2007 Published by Elsevier B.V. All rights reserved.
doi:10.1016/j.jnucmat.2007.05.039

It is probably worthwhile mentioning the difference between the materials used in the studies under ambient and high temperature–high vacuum conditions. In the latter, pure LiH was often used, either as freshly cleaved single crystal or clean polycrystalline solids. Under ambient humidity conditions LiH will not be pure, consisting of a layer of LiOH and/or Li_2O, and it has thus become acceptable to refer to 'Salt' when working with non-pure LiH. For the purposes of this work, ambient humidity conditions refers to the relatively dry conditions LiH would experience within a fuel cell or storage device, i.e. under vacuum or backfilled with an inert dry gas of low water vapour content (0–100 ppm). A comprehensive review of investigative studies into LiH hydrolysis and product decomposition has been carried out independently by Broughton [9] and Haertling et al. [10].

The initial product during LiH hydrolysis is not clear despite three decades of study. The reaction products at elevated temperature and low H_2O partial pressures, and when only monolayer coverage occurs, have been reported [1] to be Li_2O and H_2 (Eq. (1)). At ambient temperature and on exposure to high water vapour concentrations, where more than a single monolayer of H_2O coverage is possible, the products have been reported [1] to be LiOH and H_2 (Eq. (2)). Hydration of LiOH ($LiOH \cdot H_2O$) formed on the surface of LiH has been reported on exposure to excess water vapour [2,7] (Eq. (3)).

$$2LiH + H_2O \rightarrow Li_2O + 2H_2 \tag{1}$$

$$LiH + H_2O \rightarrow LiOH + H_2 \tag{2}$$

$$LiOH + H_2O \rightarrow LiOH \cdot H_2O \tag{3}$$

Both hydrolysis reactions (Eqs. (1) and (2)) are thermodynamically favourable with $\Delta G_{298} = -94\ \text{kJ mol}^{-1}$ and $\Delta G_{298} = -133\ \text{kJ mol}^{-1}$ for the formation of Li_2O and LiOH, respectively. Several studies have reported that Li_2O forms rapidly as a very thin layer on LiH during hydrolysis (Eq. (1)) [2,11,12] and that Li_2O also reacts rapidly with water vapour to form LiOH (Eq. (4)), where $\Delta G_{298} = -87\ \text{kJ mol}^{-1}$.

$$Li_2O + H_2O \rightarrow 2LiOH \tag{4}$$

The decomposition of LiOH, in the presence of LiH, has been studied, mainly under non-ambient conditions [4,7]. LiOH decomposition has been reported to occur in vacuum/dry environments due to the existence of unstable forms of LiOH which was attributed to LiOH near the LiH substrate and ambient interface. Dinh et al. [7] measured a range of activation energies for the decomposition of LiOH, which indicated that LiOH decomposed most easily near the LiH substrate, then near the ambient interface [13]. Dinh's work suggested that stable surface LiOH would also decompose when exposed to a strong water pump at elevated temperature, but at a very slow rate, which is consistent with thermodynamics where the Gibbs free energy for LiOH decomposition is positive $\Delta G_{298} = +174\ \text{kJ mol}^{-1}$. Decomposition of surface LiOH may be able to occur under ambient conditions but would require a long time to be observed. Furthermore, the continued presence of H_2O can be expected to shift the equilibrium in favour of LiOH production, thus preventing observation of Li_2O.

This work was part of a wider study [14–19] to investigate the reactions of LiH to provide the data necessary for a predictive ageing model to be developed. The development of such a model requires accurate information on the behaviour of LiH when exposed to known temperatures, pressures and water vapour (or air) exposures. A predictive model is required to support lifetime prediction studies for components or cells fabricated from LiH. Hydrolysis of LiH powder has been studied under variable water vapour exposures at ambient temperature and pressure using diffuse reflectance infrared Fourier transform (DRIFT) spectroscopy in order to understand the conditions that promote hydrolysis and the mechanisms involved. Hydrolysis rates were measured by monitoring the growth of LiOH. Li_2O was also selected for investigation because it has been identified as a possible intermediate product during hydrolysis of LiH.

2. Experimental

2.1. Materials

LiH (95% purity), Li_2O (99.5% purity) and LiOH (98% purity) were obtained from Alfa Aesar. KBr (99.99% spectroscopy grade), obtained from Aldrich, was used as the background material for DRIFT spectra and was dried at 400 °C for 24 h prior to use. All samples, including the reference material, were sieved prior to use to produce powders with a particle size range of 53–105 μm. All sample handling and preparation was performed in a dry argon (approx. 10 ppm H_2O) filled glovebox.

2.2. Equipment

DRIFT spectra were recorded using a Perkin Elmer Spectrum 1B FT-IR spectrometer with a medium-band ($7800–580\ \text{cm}^{-1}$) MCT detector. The spectrometer was coupled to a variable temperature environmental chamber (Grazeby-Specac Ltd.) and Grazeby-Specac 'Selector' diffuse reflectance mirror assembly. Prior to use, the environmental chamber was purged with dry argon and heated to 500 °C for 24 h to remove residual water vapour from within the chamber. A total of 64 scans per spectrum were continuously recorded, during a period of up to 500 min, over the spectral range $700–4000\ \text{cm}^{-1}$ at a resolution of $8\ \text{cm}^{-1}$ and scanning speed of $1\ \text{cm}^{-1}\ \text{s}^{-1}$. This equated to one spectrum collected every 38 s. The background spectra were collected at the same temperature as the DRIFT sample spectra. The background was automatically subtracted from the sample spectra. None of the samples were diluted but total absorbance kept low by utilising a small platinum sample cup (7 mm diameter × 3 mm high) for sample loading, which was placed directly into the environmental chamber sample cell.

2.3. Presentation of DRIFT spectra

DRIFT spectra have been presented as diffuse absorbance ($-\log(R/R_0)$), which is analogous to absorbance ($-\log(T/T_0)$) used in classical transmission spectroscopy. The use of reflectance ratio (R/R_0), where R_0 is a reference material, can result in poor quality spectra because strong absorption leads to small numerical values ($R/R_0 < 0.01$) [20]. Kubelka-Munk format [21] is often used as an alternative for quantitative work because the relative band intensities can be related to concentration, although this relationship is only valid for very dilute samples. Kubelka-Munk format tends to accentuate stronger bands at the expense of weaker bands in graphical representations, making DRIFT spectra appear flat and almost featureless. Consequently, the use of Kubelka-Munk format was not considered appropriate for this work. The hydrolysis rate of LiH was measured using the LiOH hydroxyl band located at 3676 cm^{-1} during exposure to known concentrations of water vapour.

3. Results and discussion

3.1. DRIFT spectra of LiH and hydrolysis products

The DRIFT spectra of lithium hydride powder showed two distinct infrared absorption bands: a broad band centred at 1280 cm^{-1} (LiH) and a sharp band centred at 3676 cm^{-1} (OH) as shown in Fig. 1. The O–H band was attributed to formation of LiOH due to the reaction of the sample surface with trace amounts of water vapour present in the glovebox in which the material was handled (nominally 10 ppm H_2O). All spectra of LiH obtained during this work indicated the presence of LiOH, which was inherent in the as-supplied material. Ren [8] reported commercial quality LiH typically containing up to 6 vol.% LiOH. Only under conditions of ultra-high vacuum whilst using cleaved single crystals [7] it is possible to achieve a completely clean LiH sample free of LiOH contamination.

The DRIFT spectrum of Li_2O contained the strong Li–O band at 850 cm^{-1} and surface LiOH was detected at 3676 cm^{-1} due to hydrolysis of Li_2O. The spectrum for Li_2O is very similar in appearance to that of LiH (Fig. 1), except for the shift in the Li–X peak position (where X = H or O), and is therefore not shown.

3.2. Hydrolysis during water vapour exposure

3.2.1. Lithium hydride

Water vapour was introduced to the sample chamber by flowing dry argon through a purpose-made [9] moisture blending system, and allowing the moist gas to flow at constant rate (100 $\text{cm}^3\,\text{min}^{-1}$) over the sample. Samples were exposed to environments including dry flowing gas, 2% RH (64 Pa), 50% RH (1585 Pa) and in excess of 60% RH (1900 Pa).

The hydroxyl band at 3676 cm^{-1} in the water vapour-exposed samples indicated hydrolysis, with an initially rapid rate followed by a slower and steadier rate (Fig. 2). The initial rate on exposure of LiH to 2% RH (64 Pa) water vapour was almost half the rate observed on exposure at 50% RH (1585 Pa) (0.09 compared with 0.05 absorbance units per minute, respectively). The difference in initial hydrolysis rates and the slowing of the subsequent hydrolysis rate was attributed to the relatively slow formation of a coherent layer of LiOH on the surface of the sample (Fig. 3). This LiOH layer was considered to inhibit, but

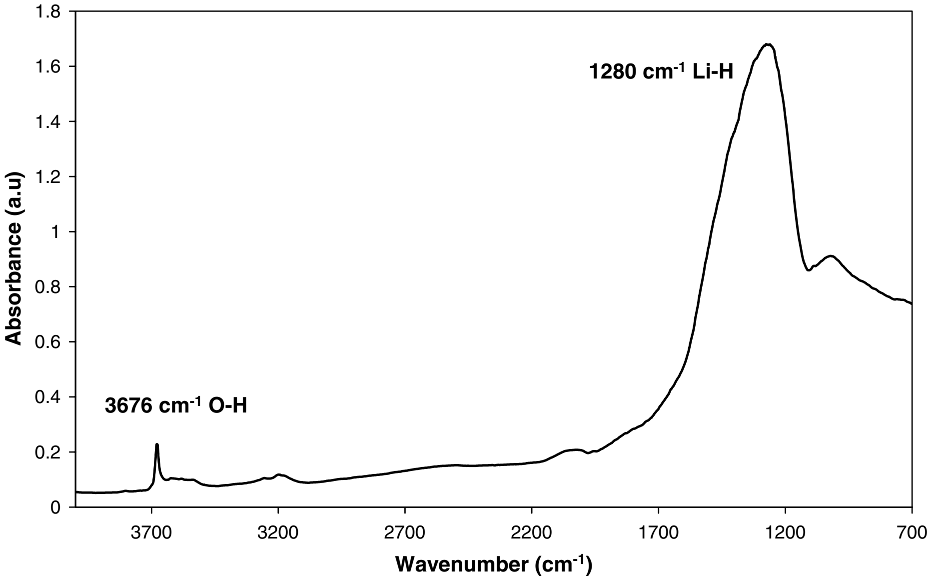

Fig. 1. Typical DRIFT spectrum of LiH showing evidence of exposure to water vapour in the form of the hydroxyl stretching band at 3676 cm^{-1}.

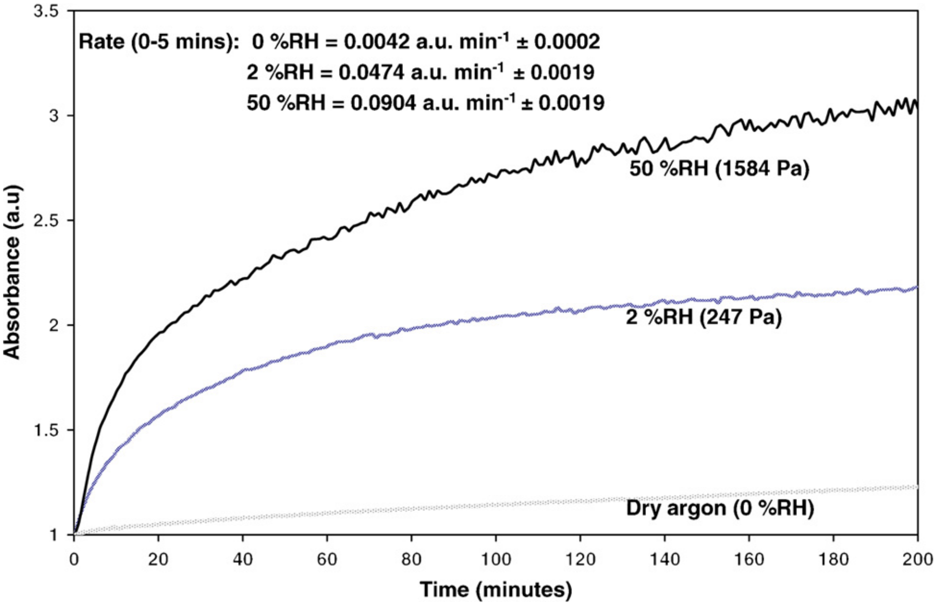

Fig. 2. Hydrolysis rates (measured at 3676 cm^{-1}) of LiH showing that the rate of hydrolysis at 2% RH is only half of that observed at 50% RH but is still significant. The reduced rate at 2% RH was attributed to the formation of a coherent passivating layer of LiOH on the LiH surface.

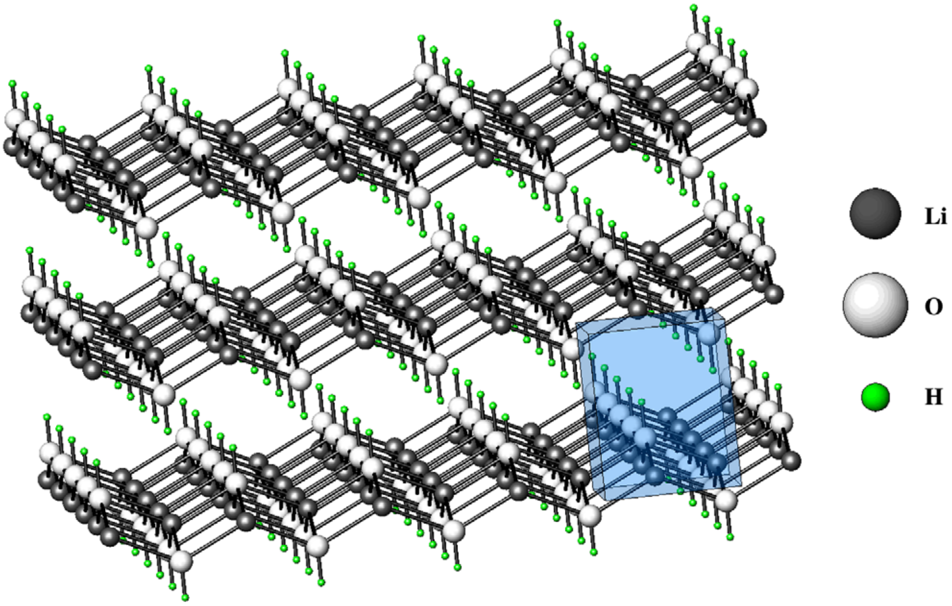

Fig. 3. Graphical representation of the coherent layer structure of LiOH.

not prevent, further reaction of LiH with water vapour resulting in the reduced hydrolysis rate. At 50% RH (1585 Pa) exposure, the signal to noise ratio (SNR) reduced after approximately 40 min, and was attributed to the sample surface beginning to swell or produce cracks and fissures as the LiOH layer grew on the surface. Swelling of the sample surface resulted in the IR beam becoming out-of-focus with the original sample surface, leading to a reduction in SNR. The reduction in SNR was not as pronounced at 2% RH (64 Pa) and negligible under nominally dry argon, where the water vapour concentration was approximately 10 ppm. Fig. 2 shows that reaction with water vapour is fastest during the initial stages of exposure, and that the level of water vapour exposure determines the thickness of the LiOH corrosion layer, and hence the ability of this layer to inhibit further reaction with water vapour.

During exposure of LiH powder to nominally dry argon (~10 ppm H_2O), hydrolysis was still observed, but did not show the initial rapid rate as seen with water vapour exposures. A near linear rate was observed, 10 times less than that observed at 2% RH (64 Pa) exposure (0.0042 absorbance units per minute). Hydrolysis under dry flow gas conditions was not expected, but analysis indicated that some residual water vapour may have been adsorbed within the gas delivery system which was not subjected to pre-heating under vacuum. Therefore, adsorbed water being carried along with the flow gas allowed limited hydrolysis of the sample.

These results (Fig. 2) show that hydrolysis of LiH can occur even under nominally dry conditions, resulting in formation of LiOH at the sample surface. This confirmed the need to use ultra-high vacuum and bake-out regimes on any equipment in which LiH will come into contact. Even under relatively dry conditions of 2% RH (64 Pa) the rate of hydrolysis was significant.

No bands associated with Li_2O or $LiOH \cdot H_2O$ were detected on exposure of LiH up to and including 50% RH (1584 Pa), even after exposure times of 150 min (Fig. 4). Only LiOH was detected as a hydrolysis product despite the phase diagram (Fig. 5) for the LiH system suggesting the formation of $LiOH \cdot H_2O$ at 15% RH (476 Pa). It is possible that DRIFT did not have the sensitivity to detect a very thin layer of $LiOH \cdot H_2O$ on the surface of LiH or LiOH or a thin layer of Li_2O between LiH and LiOH. However, the $LiOH \cdot H_2O$ band at 3570 cm^{-1} was expected to be relatively intense and well resolved. The detection of very thin layers of Li_2O, which will produce very weak absorption bands, may not be possible due to interference from the strong LiH band nearby, and also due to absorption or scattering of radiation from the Li_2O layer by any absorbing layer of LiOH above it. It

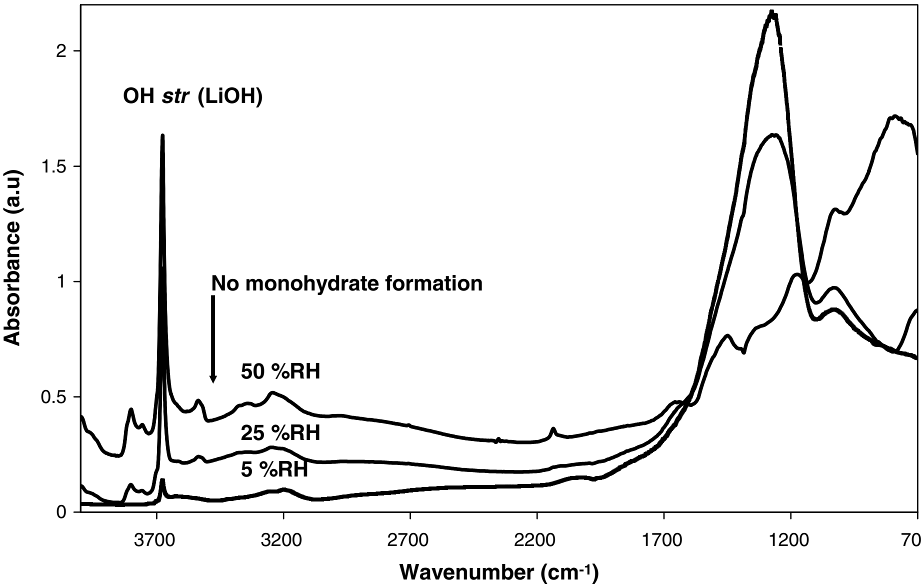

Fig. 4. DRIFT spectra of LiH after 150 min exposure to relative humidity's of 5%, 25% and 50%. This showed that exposures of up to 50% RH did not result in the formation of $LiOH \cdot H_2O$.

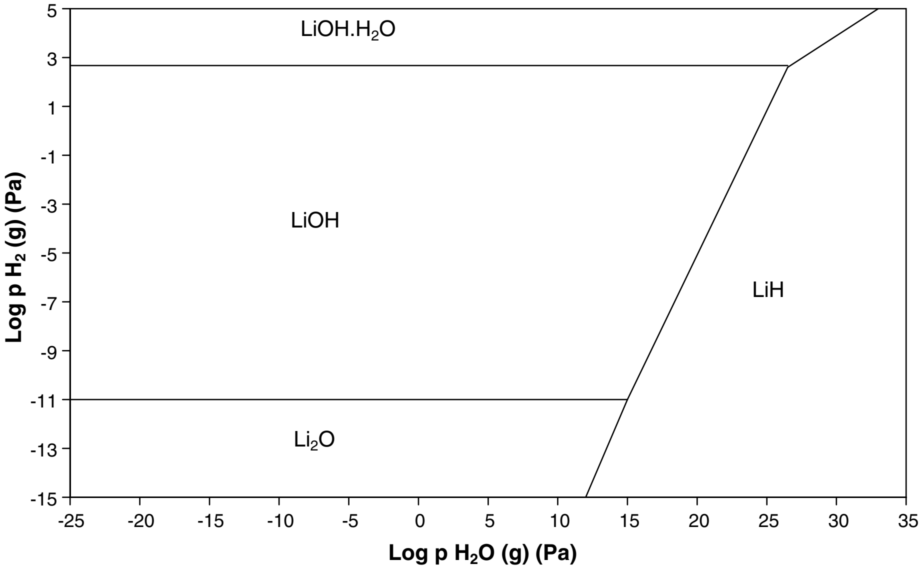

Fig. 5. Phase diagram for LiH hydrolysis products at 25 °C.

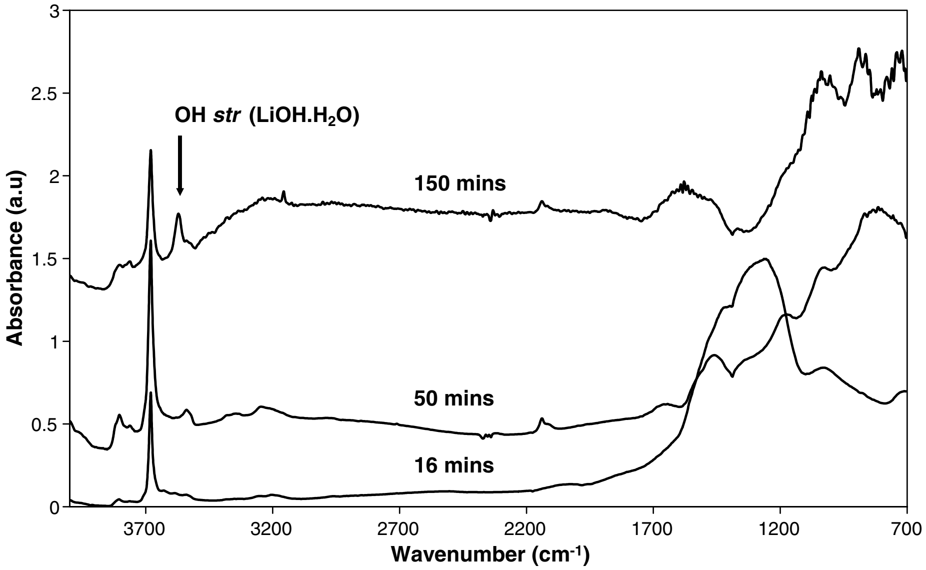

Fig. 6. DRIFT spectra of LiH during exposure to 60% RH environment showing formation of $LiOH \cdot H_2O$ only after 100 min exposure.

has been suggested that the Li_2O layer, during hydrolysis of LiH, may be approximately 10 nm thick [22], which suggests that DRIFT is not sensitive enough or capable of detecting such a thin, sub-surface product.

Satellite bands were observed either side of the hydroxyl band at 3676 cm^{-1}, which were associated with overtones caused by minor exposure to CO_2 probably as a result of dissolved CO_2 in the water used in the moisture blending system.

The DRIFT spectrum of LiH exposed to water vapour in excess of 50% RH showed evidence of $LiOH \cdot H_2O$ (Fig. 6). In addition to the expected OH stretching band at 3676 cm^{-1} a further sharp band was observed at 3570 cm^{-1}, which was attributed to OH stretching of the hydroxyl in LiOH bound to water. This band formed along with a broad band between 3500 and 2700 cm^{-1} due to hydrogen bonding. It was not possible to obtain a good quality DRIFT spectrum of pure $LiOH \cdot H_2O$ due to the material agglomerating into larger particles and causing increased specular reflectance and subsequent distortion of the spectrum [23–29]. The spectral distortion was observed below 1700 cm^{-1} where some bands appeared inverted. Dehydration of water vapour-exposed LiH and Li_2O, by the application of vacuum or heating above 100 °C, resulted in the removal all bands associated with $LiOH \cdot H_2O$.

3.2.2. Lithium oxide

In contrast to LiH, the spectra of Li_2O obtained during constant exposure to water vapour at 25% RH (792 Pa) (Fig. 7) shows that $LiOH \cdot H_2O$ formed within the first minute as indicated by the appearance of a sharp band at 3570 cm^{-1} along with the broad H-bonding band from 3500 to 2700 cm^{-1}. The spectra not only show bands associated with $LiOH \cdot H_2O$ but also has the sharp hydroxyl band at 3676 cm^{-1}. This was expected, given that hydrolysis of Li_2O must initially produce anhydrous LiOH before formation of the hydrated hydroxide. Experiments confirmed that even on exposure to 2% RH (64 Pa) $LiOH \cdot H_2O$ was detected within 1 min.

The rapid formation of $LiOH \cdot H_2O$ during hydrolysis of Li_2O was not observed during hydrolysis of LiH, indicating that the reaction balance differed significantly despite both materials initially hydrolysing to LiOH. Li_2O could not be detected in the DRIFT spectra of LiH but its presence could potentially be inferred from the rapid formation of $LiOH \cdot H_2O$, assuming that Li_2O on LiH would convert to LiOH and become hydrated very quickly. However, LiH did not exhibit any bands associated with $LiOH \cdot H_2O$, except when exposed to high levels of water vapour for long periods where the surface layer of LiOH could become saturated. The absence of Li_2O or $LiOH \cdot H_2O$ suggests that Li_2O cannot be detected during LiH hydrolysis and that the mechanism of hydrolysis of Li_2O in the absence of LiH is significantly different to that of pure Li_2O alone.

The difference in reactivity and formation of $LiOH \cdot H_2O$ can be explained by considering the effect LiH may have on the reactions involving LiOH. The hydrolysis of Li_2O in the absence of LiH is illustrated in Fig. 8 and shows that on exposure to water vapour Li_2O can only form LiOH, which may become hydrated as soon as it is formed. LiH may also hydrolyse to LiOH (even if *via* Li_2O) but a reaction between LiH and LiOH or decomposition of LiOH may also occur, although at a slower rate than hydrolysis, yielding more Li_2O, as illustrated in Fig. 9. This product may then react with water vapour to produce LiOH and continue as a regenerating cycle preventing formation of $LiOH \cdot H_2O$ except under conditions of excess water vapour or once all the available LiH has been used. Because of the absence of LiH, Li_2O alone cannot undergo such a cycle and hence was observed to pref-

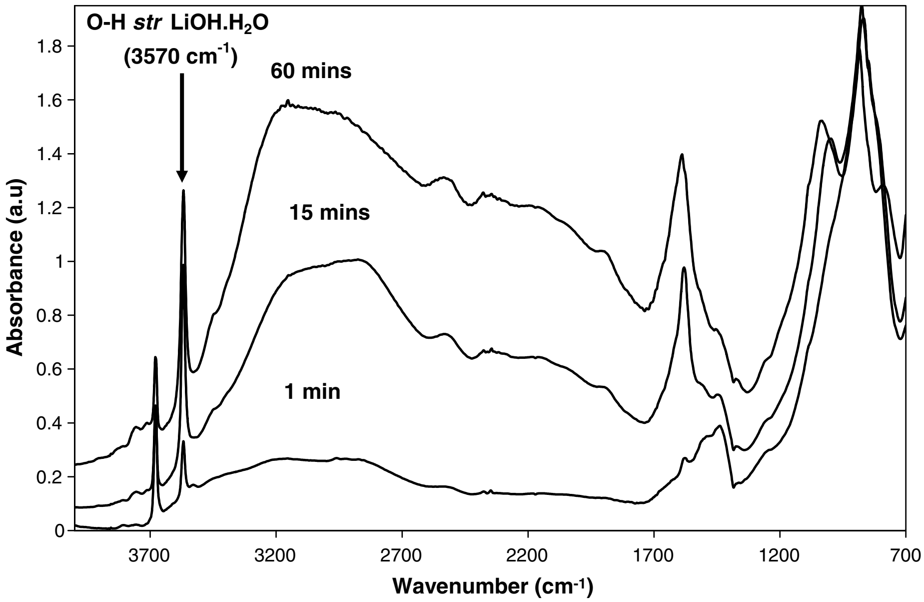

Fig. 7. DRIFT spectra of Li_2O as observed during 60 min of exposure to 25% RH environment. Formation of $LiOH \cdot H_2O$ was observed within the first minute as noted by the appearance of the band at 3570 cm^{-1}.

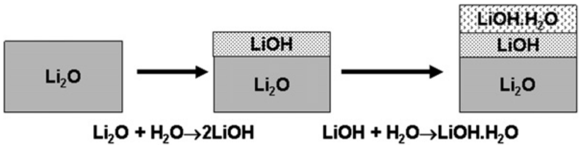

Fig. 8. Schematic illustration of the hydrolysis of Li_2O in the absence of LiH.

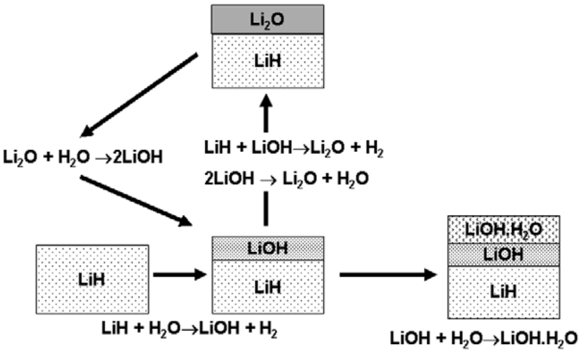

Fig. 9. Schematic illustration of the LiH hydrolysis mechanisms when exposed to water vapour under ambient conditions. Production of LiOH can form directly, or via a Li_2O intermediate. Li_2O can also form from the solid-state reaction between LiH and LiOH.

erentially form $LiOH \cdot H_2O$ on exposure to even small amounts of water vapour.

3.3. LiH hydrolysis reactions and mechanisms

This rapid conversion of Li_2O to LiOH at the surface has made positive identification of Li_2O as an initial hydrolysis product impossible using DRIFT spectroscopy. Other recent work using X-ray diffraction [8] also failed to positively identify Li_2O on a LiH surface. This was despite studying LiH under conditions of minimal exposure to H_2O and O_2, and after brief air exposure. This suggests that if Li_2O was formed as an initial hydrolysis product under ambient humidity conditions then its reaction with water is so rapid, as has been previously suggested [1], that Li_2O is instantly converted to LiOH. A phase diagram [30] (Fig. 5) of the LiH system shows that only at very low partial pressures of water vapour will Li_2O form and, as the partial pressure increases, the predominant product will be LiOH. Above 15% RH (476 Pa) at room temperature the most stable product is $LiOH \cdot H_2O$. Given the difficulty in observing the formation of Li_2O at the LiH surface it is suggested that its formation is extremely rapid and only forms a very thin layer before quickly hydrolysing to LiOH.

Although Li_2O has not been observed at the surface of LiH under ambient humidity conditions, it has been observed within the LiH bulk [2,11,31,32] as a sub-layer between LiH and LiOH. The Li_2O layer has been reported to be only 10 nm [22] and is a result of a solid-state reaction between LiH and LiOH (Eq. (5)) [3,4,12]. This work showed no evidence of Li_2O, but the duration of the experiments were likely to be too short to allow a solid-state reaction to occur to such an extent that the oxide product could be detected. The solid-state reaction between LiH and LiOH is thermodynamically favourable ($\Delta G_{298} = -55\ kJ\ mol^{-1}$) but is unlikely to proceed at a significant rate compared with the hydrolysis of LiH and Li_2O. Furthermore, the LiH band (1280 cm^{-1}) in DRIFT spectra is very intense and broad and close to where the very weak Li_2O band would appear (850 cm^{-1}), therefore it is unlikely the Li_2O band would be resolvable in the presence of LiH.

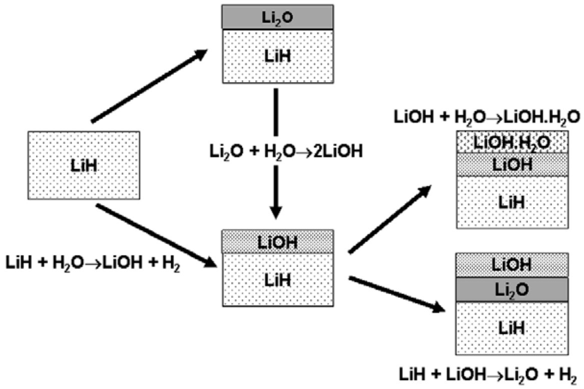

Fig. 10. Schematic illustration of the hydrolysis mechanisms on LiH on exposure to high and low concentrations of water vapour.

Therefore, it is probable that any oxide layer formed between LiH and LiOH cannot be detected with this technique.

$$LiOH + LiH \rightarrow Li_2O + H_2 \tag{5}$$

Under long periods of storage, or elevated temperature, LiOH may decompose slowly and result in a surface layer of Li_2O, but under normal ambient conditions, and where water vapour is available, it is unlikely this product would be observed. A reaction scheme is illustrated in Fig. 10 which describes the likely reactions that occur when LiH is exposed to water vapour and considers the product of the solid-state reaction between LiH and LiOH.

4. Conclusions

The shape of the hydroxyl growth curves presented in this paper are typical of hydrogen growth profiles [6] for this type of material, with a rapid initial rate followed by a slower rate that tends towards zero. The initially rapid rate is attributed to the formation of LiOH at the LiH surface. The slowing of the rate of OH production is attributed to the build-up of a thickening layer of LiOH. At low levels of water vapour exposure (2% RH, 64 Pa) this layer formed more slowly than when compared with much higher exposures and suggested the formation of a possibly more coherent passivating layer. This is reflected in the differences in the hydroxyl growth profiles at 2% RH and 50% RH exposures where the initial rate at 50% RH is almost two times the rate at 2% RH.

Thermodynamics suggested that the initial reaction produces Li_2O, which converts to LiOH on hydrolysis. This work, under ambient conditions, found no evidence of Li_2O on the surface of LiH, but its formation may have been masked by the rapid rate of hydrolysis of both LiH and Li_2O. This suggested that Li_2O, if formed initially, only existed briefly before being hydrolysed to LiOH and that decomposition of LiOH at the LiH surface had not occurred. Li_2O produced from a solid-state reaction between LiH and LiOH was not detected by DRIFT spectroscopy, principally because the product was likely to be below the surface and inaccessible using this technique. It was also considered that, despite being thermodynamically favourable, Li_2O from a solid-state reaction at ambient temperature would be produced very slowly and would therefore not be produced in any measurable quantities.

Lithium oxide was observed to hydrolyse rapidly on exposure to water vapour, even at trace levels, to produce $LiOH \cdot H_2O$. This product was not detected during hydrolysis of LiH, except at exposures greater than 50% RH and then only after prolonged exposure. This supported the conclusion that LiH hydrolysis did not yield a stable surface product of Li_2O, but did not discount its formation on initial H_2O exposure.

Acknowledgements

The author would like to thank Professor Ian A. Donald, Dr Jon S. Joy, David M. Grant and Kim J. Bartram (AWE plc) for their valuable comments and discussion offered during the preparation of this work.

References

[1] W.D. Machin, F.C. Tompkins, Trans. Faraday Soc. 62 (1966) 2205.
[2] C.E. Holcombe, G.L. Powell, J. Nucl. Mater. 47 (1973) 4320.
[3] J.J. Vajo, S.L. Skeith, F. Mertens, S.W. Jorgensen, J. Alloys Compd. 390 (2005) 55.
[4] L.N. Dinh, D.M. Grant, M.A. Schildbach, R.A. Smith, W.J. Siekhaus, B. Balazs, J.H. Leckey, J.R. Kirkpatrick, W. McLean-II, J. Nucl. Mater. 347 (2005) 31.
[5] V.C.Y. Kong, F.R. Foulkes, D.W. Kirk, J.T. Hinatsu, Int. J. Hydrogen Energ. 24 (1999) 665.
[6] V.C.Y. Kong, D.W. Kirk, F.R. Foulkes, J.T. Hinatsu, Int. J. Hydrogen Energ. 28 (2003) 205.
[7] L.N. Dinh, C.M. Cecala, J.H. Leckey, M. Balooch, J. Nucl. Mater. 295 (2001) 193.
[8] R. Ren, A.L. Ortiz, T. Markmaitree, W. Osborn, L.L. Shaw, J. Phys. Chem. B 110 (2006) 10567.
[9] D.A. Broughton, Hydrolysis of Lithium Hydride, PhD Thesis, University of Reading, UK, 2001.
[10] C. Haertling, R.J. Hanrahan, R. Smith, J. Nucl. Mater. 349 (2006) 195.
[11] S. Cristy, SIMS depth profiling of an insulating air-sensitive material, Report No. Y/DW-725, Oak Ridge, Y-12 Plant, US, 1987.
[12] S.M. Myers, J. Appl. Phys. 45 (1974) 4320.
[13] J.E. Keister (Ed.), Nuclear Materials Research Developments (Chapter 6: Hydrogen outgassing in lithium hydride), Nova Publishers Inc., New York, ISBN 1-60021-432-0, in press.
[14] D.A. Broughton, in: 13th International Meeting on NMR Spectroscopy, University of Exeter, UK, 1997.
[15] D.A. Broughton, in: International Conference on Ageing Studies and Lifetime Extension of Materials, Oxford University, 1999.
[16] R.P. Awbery, Infrared Study of Lithium Hydride and Deuteride by Diffuse Reflectance, MSc thesis, Reading University, 2004.
[17] D.A. Broughton, R.P. Awbery, J.S. Joy, in: 4th International Conference on Inorganic Materials, University of Antwerp, Belgium, 2004.
[18] J.S. Joy, in: CIMTEC International Conference, Acireale, Sicily, 2006.
[19] R.P. Awbery, in: 5th International Conference on Inorganic Materials, Ljubljana, Slovenia, 2006.
[20] N.R. Smyrl, E.L. Fuller, G.L. Powell, Appl. Spectrosc. 37 (1983) 38.

[21] G. Kortum, Reflectance Spectroscopy, Springer-Verlag, New York, 1969.
[22] C.L. Haertling, R.J. Hanrahan, J.R. Tesmer, J. Phys. Chem. C 111 (2007) 1716.
[23] P.W. Yang, H.H. Mantsch, Appl. Optics 26 (1987) 326.
[24] W. Maddams, Int. J. Vib. Spectrosc. [www.ijvs.com] 1,1,3, 1996.
[25] P.J. Brimmer, P.R. Griffiths, Anal. Chem. 58 (1986) 2179.
[26] D.M. Hembree, H.R. Smyrl, Appl. Spectrosc. 43 (1989) 267.
[27] M.P. Fuller, P.R. Griffiths, Anal. Chem. 50 (1978) 1906.
[28] D.J.J. Fraser, P.R. Griffiths, Appl. Spectrosc. 44 (1990) 193.
[29] T. Iwaoka, S.-H. Wang, P.R. Griffiths, Spectrochim. Acta 41A (1985) 37.
[30] HSC Thermodynamics and Equilibrium Constants, Outokumpu Research Oy, Finland, 2000.
[31] J. McLaughlin, S. Cristy, Composition of corrosion films on lithium hydride surfaces after exposure to air, Report No. Y-1929, Oak Ridge, Y-12 Plant, US, 1974.
[32] S. Myers, J. Appl. Phys. 47 (1974) 121.